Supplementary materials: Measuring the impact of Ebola control measures in Sierra Leone

Adam J. Kucharski[1], Anton Camacho[1], Stefan Flasche[1], Rebecca E. Glover[1], W. John Edmunds[1], Sebastian Funk[1]

[1] Centre for the Mathematical Modelling of Infectious Diseases, Department of Infectious Disease Epidemiology, London School of Hygiene & Tropical Medicine

S1 Estimation of duration of infectiousness

The duration of infectiousness, $1/\gamma$, was first calculated separately for cases that result in death and recovery. For cases that resulted in death, the duration of infectiousness was calculated as the reported average duration from onset-to-death (8.6 days) [1] plus one day for burial for cases that were not ascertained (1-r) [2]. For cases that recovered, we used the duration from onset-to-hospital discharge (17.2 days) [1] minus 48 hours, as this is the time that would have elapsed since first possible confirmation that the patient was no longer infectious (to be discharged, a patient must test negative for Ebola twice, with an interval of 48 hours between tests [3]). We then combined the two estimates, weighting by the case fatality rate (69%) [1]:

$$1/\gamma = 0.69 \times (8.6 + (1 - r)) + (1 - 0.69) \times (17.2 - 2) \quad \text{(S1)}$$

In our main analysis 60% of cases were ascertained, and hence $1/\gamma$=10.9 days. As a sensitivity analysis we also considered an infectious period of 9 days, equal to the reported average duration from onset-to-death (8.6 days) plus one day for burial for cases that were not ascertained (under 60% ascertainment).

By a similar calculation, the average from onset-to-outcome for cases that seek treatment was $0.69 \times 8.6 + (1 - 0.69) \times (17.2) = 11.3$ days. This value was used to estimate average duration of stay in EHC/CCC/ETU (Table S1).

References

[1] WHO Ebola Response Team (2014) Ebola virus disease in West Africa — the first 9 months of the epidemic and forward projections. *New England Journal of Medicine* 371:1481–1495.

[2] Nielsen CF, et al. (2015) Improving Burial Practices and Cemetery Management During an Ebola Virus Disease Epidemic. Sierra Leone, 2014. *MMWR. Morbidity and mortality weekly report* 64:20–27.

[3] World Health Organisation (2015) Criteria for declaring the end of the Ebola outbreak in Guinea, Liberia or Sierra Leone. *http://www.who.int/csr/disease/ebola/declaration-ebola-end/en/*.

[4] Breman J, et al. (1978) The epidemiology of Ebola hemorrhagic fever in Zaire, 1976. *Ebola virus haemorrhagic fever (Pattyn, SR ed.)* pp 85–97.

[5] Bentley N (2015) Sierra Leone Ebola labs project – beating the outbreak at source. *Public Health England Blog*.

[6] World Health Organisation (2015) Ebola response roadmap situation reports. *apps.who.int/ebola/en/current-situation/ebola-situation-report-20-may-2015*.

Supplementary Tables

Table S1: Parameter definitions and values.

Parameter	Definition	Value	Reference
$1/\nu$	Latent period	9.4 days	[1, 4]
$1/\gamma$	Mean duration of infectiousness	10.9 days	See supplementary text
$1/\tau_H$	Mean time from onset of symptoms to EHC/CCC admission	1.8 to 4.6 days	See Fig. S1
$1/\tau_U$	Mean time spent in EHC/CCC awaiting test results	2 days	[5]
$1/\tau_D$	Mean duration of stay in ETU	$11.3-1/\tau_H - 1/\tau_U$	
$1/\tau_F$	Mean duration of stay in EHC/CCC if no ETU beds	$11.3-1/\tau_H$	
$1/\nu$	Mean time from onset of symptoms to case report	4.5 days	[1]
r	Proportion of cases that are ascertained	0.4, 0.6, 0.8	
$\hat{\beta}$	Initial transmission rate	Estimated	
a_1	Slope of change in transmission rate	Estimated	
a_2	Final value of transmission rate	Estimated	
a_τ	Midpoint of time of change in transmission rate	Estimated	
σ	Volatility of transmission rate	Estimated	
ϕ	Overdispersion of reporting process	Estimated	

Table S2: Relationship between relative reduction in R_0, initial R_0, and total cases per 100,000 population in each district. Relative reduction in R_0 is calculated as $1 - R_0^T/R_0^0$, where R_0^0 is the median basic reproduction number at the start of the period of study, and R_0^T is the median basic reproduction number on 2nd February 2015. Association between reduction and the other two variables was tested using Pearson's product moment correlation coefficient.

District	Relative reduction in R_0	Initial R_0	Cases/100,000
Pujehun	-8.74E-11	0.546	12.7
Koinadugu	-2.52E-15	0.792	62.1
Bo	1.52E-08	1.76	89.7
Kambia	0.000795	1.98	69.1
Tonkolili	0.00158	1.31	179
Moyamba	0.00281	1.1	107
Port Loko	0.0661	1.55	437
Kono	0.148	1.81	151
Kenema	0.299	2.39	114
Western Area	0.378	2.41	395
Bombali	0.553	3.36	264
Kailahun	0.604	3.31	206
	Correlation:	0.905	0.445
	p-value:	$<$0.0001	0.147

Table S3: Estimated number of cases averted up to 2nd February 2015 as a result of additional treatment beds, when $1/\gamma$=10.9 days and 80% cases are ascertained.

District	Initial R_0	Beds introduced	Additional beds	Beds 4 weeks earlier
Bo	1.8 (1.6–2.3)	124	14,600 (388–39,000)	15,100 (423–89,700)
Bombali	3.4 (2.2–5.2)	506	8,570 (4–73,400)	12,500 (2–207,000)
Kailahun	3.3 (2.9–3.8)	123	20,500 (12,200–36,900)	21,400 (13,200–37,700)
Kambia	2.0 (1.4–9.6)	55	532 (0–4,970)	679 (0–20,000)
Kenema	2.4 (1.7–4.0)	75	274 (199–411)	440 (304–635)
Koinadugu	0.8 (0.6–1.2)	92	62 (26–189)	144 (79–290)
Kono	1.8 (1.5–16.2)	83	1,730 (0–3,580)	2,440 (0–7,810)
Moyamba	1.1 (0.9–5.4)	34	138 (72–253)	243 (153–442)
Port Loko	1.6 (1.5–1.7)	546	8,410 (5,680–11,600)	10,300 (7,160–14,200)
Pujehun	0.5 (0.4–1.0)	24	12 (5–41)	25 (12–58)
Tonkolili	1.3 (1.1–2.8)	349	1,300 (10–8,470)	1,680 (18–12,000)
Western Area	2.4 (2.3–2.6)	960	82,800 (67,100–109,000)	89,200 (73,300–114,000)
Total		2971	148,000 (115,000–219,000)	159,000 (126,000–351,000)

Table S4: Estimated number of cases averted up to 2nd February 2015 as a result of reduction in community transmission and/or additional treatment beds, when $1/\gamma$=10.9 days and 40% cases are ascertained.

District	Initial R_0	Beds introduced	Additional beds	Beds 4 weeks earlier
Bo	1.9 (1.4–3.2)	124	2,150 (1,140–4,670)	2,770 (1,430–8,580)
Bombali	4.1 (3.3–5.7)	506	3,460 (2,960–4,270)	4,600 (4,000–5,570)
Kailahun	6.2 (1.7–11.5)	123	1,420 (0–9,520)	2,430 (1–22,800)
Kambia	1.4 (1.2–1.5)	55	432 (295–578)	641 (446–816)
Kenema	2.2 (1–14.7)	75	120 (0–12,700)	181 (0–18,400)
Koinadugu	0.6 (0.3–0.9)	92	29 (12–96)	95 (51–208)
Kono	3.5 (1.3–19.3)	83	78 (0–3,020)	132 (0–8,600)
Moyamba	1.1 (0.8–12.2)	34	97 (0–549)	187 (0–1,340)
Port Loko	2.3 (1.8–3.0)	546	2,450 (369–6,980)	4,230 (629–12,600)
Pujehun	0.5 (0.3–1.4)	24	9 (2–28)	23 (9–51)
Tonkolili	2.9 (1.7–6.6)	349	400 (133–850)	788 (292–1,660)
Western Area	2.5 (2.3–2.9)	960	17,600 (14,600–20,900)	25,000 (19,800–28,700)
Total		2971	29,200 (24,500–47,700)	42,600 (34,700–75,000)

Table S5: Estimated number of cases averted up to 2nd February 2015 as a result of additional treatment beds, when $1/\gamma$=9 days and 60% cases are ascertained.

District	Initial R_0	Beds introduced	Additional beds	Beds 4 weeks earlier
Bo	1.6 (1.4–2)	124	5,170 (2,710–8,920)	5,700 (3,270–9,460)
Bombali	5.7 (3.8–8.2)	506	5,640 (4,720–6,900)	6,720 (5,800–7,940)
Kailahun	6 (4.1–14.8)	123	3,550 (1,830–5,880)	4,330 (2,940–6,770)
Kambia	1.5 (1.2–3)	55	547 (89–2,570)	745 (132–6,900)
Kenema	3.5 (1.4–14.4)	75	0 (0–31,300)	1 (0–47,700)
Koinadugu	0.7 (0.4–2.3)	92	31 (9–121)	95 (42–222)
Kono	1.6 (1.4–12)	83	1,180 (0–4,220)	1,640 (0–12,700)
Moyamba	1.1 (0.7–6.6)	34	121 (0–1,380)	224 (0–2,590)
Port Loko	1.7 (1.4–2)	546	3,960 (3,250–5,080)	5,760 (4,960–7,120)
Pujehun	0.6 (0.3–0.8)	24	10 (2–27)	21 (8–47)
Tonkolili	2.8 (1.4–6.8)	349	571 (370–846)	956 (689–1,290)
Western Area	2.3 (2.1–2.6)	960	33,100 (26,200–41,200)	39,500 (32,500–47,200)
Total		2971	54,800 (45,400–79,100)	67,500 (58,500–118,000)

Table S6: Estimated number of cases averted up to 2nd February 2015 as a result of additional treatment beds, when districts have additional imported cases. These extra cases are added to the I_t^A and I_t^N compartments in the model (weighted by the ascertainment rate, r) at an average rate of either one per day or one per week. We assume $1/\gamma$=10.9 days and 60% cases are ascertained.

District	Initial R_0	Beds introduced	With one imported case per day	With one imported case per week
Bo	1.6 (1.4–1.7)	124	8,450 (5,600–13,100)	6,680 (4,320–10,500)
Bombali	5.2 (2.9–7.9)	506	14,300 (3,850–18,400)	10,500 (1,090–16,100)
Kailahun	8.4 (5.3–16.2)	123	5,070 (2,900–9,190)	3,960 (2,190–7,090)
Kambia	1.5 (1.4–3.6)	55	936 (13–3,260)	612 (13–4,180)
Kenema	7.4 (2.1–19.4)	75	2 (0–12,700)	1 (0–16,200)
Koinadugu	0.7 (0.3–1.1)	92	49 (19–170)	39 (14–114)
Kono	1.6 (1.4–1.9)	83	1,930 (1,030–2,980)	1,610 (941–2,480)
Moyamba	1 (0.9–1.2)	34	145 (89–231)	125 (77–205)
Port Loko	1.8 (1.6–2.2)	546	4,210 (1,280–9,380)	3,900 (1,060–15,300)
Pujehun	0.5 (0.2–1.2)	24	19 (3–46)	11 (3–43)
Tonkolili	3.5 (1.3–8.4)	349	780 (61–2,710)	601 (28–4,610)
Western Area	2.5 (2.2–2.8)	960	35,600 (27,600–46,500)	33,100 (25,300–42,300)
Total		2971	72,900 (61,700–87,900)	64,900 (49,800–93,100)

Supplementary Figures

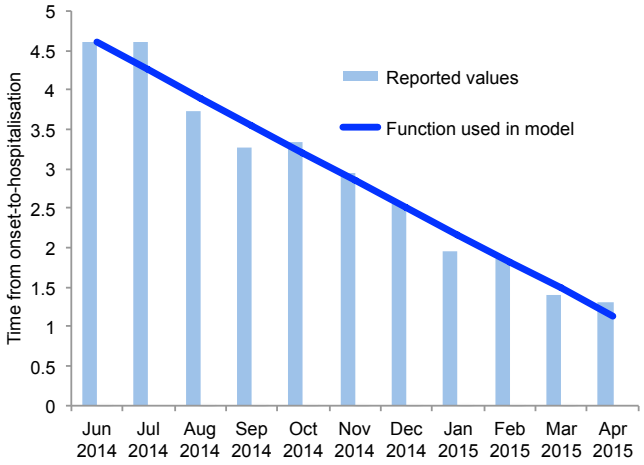

Figure S1: Decline in time from onset-to-isolation. We assume the delay in June and July 2014 was equal to the average value reported in an early summary analysis [1]; the remaining values come from WHO situation reports [6]. We used linear regression to obtain the continuos-time function used in the model.

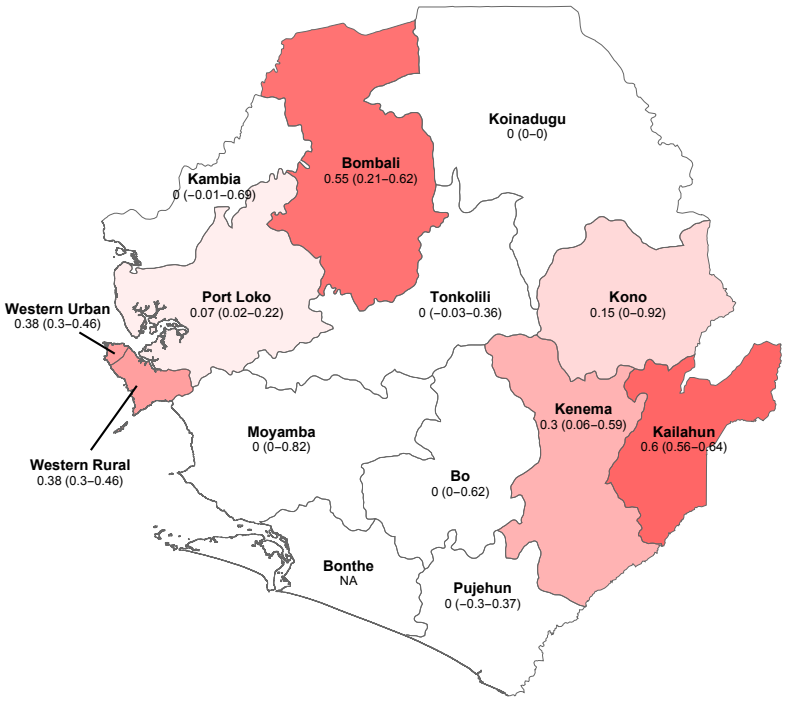

Figure S2: Relative reduction in R_0 in different districts. This is calculated as $1 - R_0^T / R_0^0$, where R_0^0 is the basic reproduction number at the start of the period of study, and R_0^T is the basic reproduction number on 2nd February 2015. Districts are coloured by median reduction in R_0, the value for which is given below the district name (95% credible intervals are in parentheses). In the model we treated the two parts of Western Area (Urban and Rural) as one district, as this is how case data were typically reported. There was no estimate of reduction in Bonthe, as we did not fit the model to this district (see main text for details). District boundaries obtained from the GADM database of Global Administrative Areas, freely available from *http://www.gadm.org* .

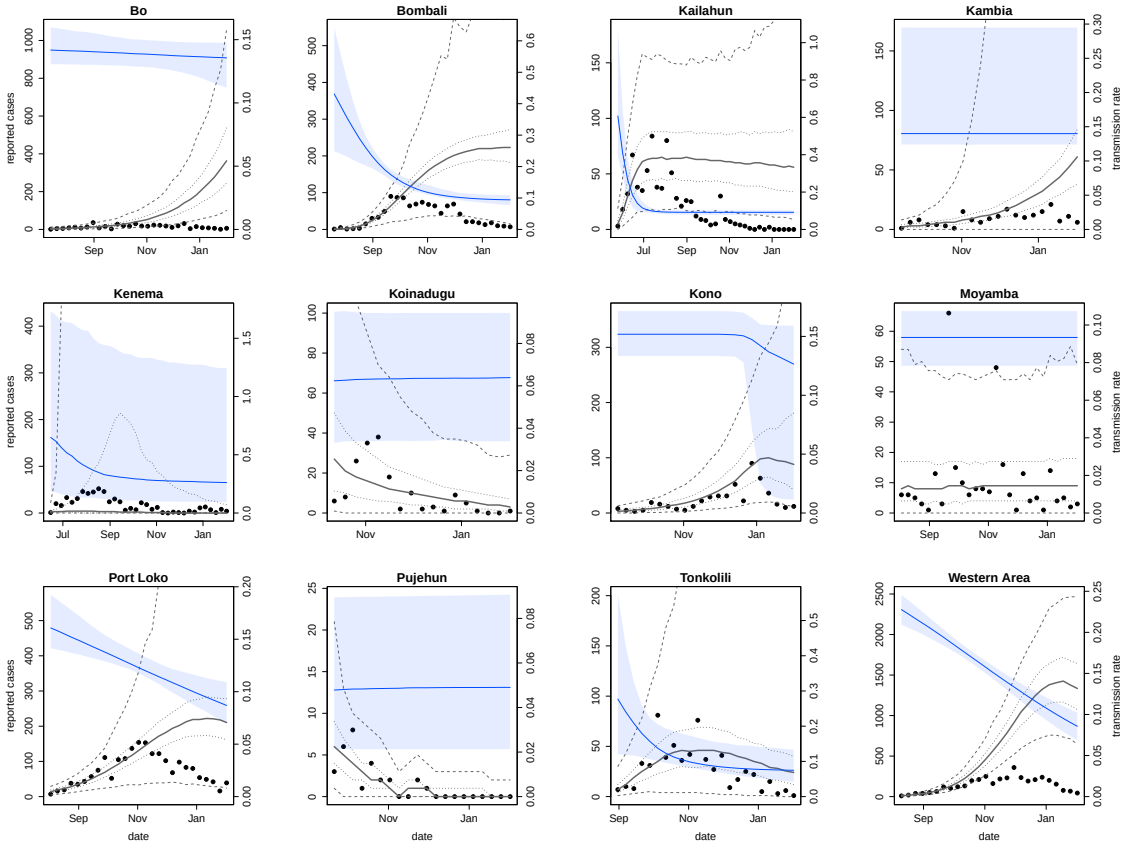

Figure S3: District-level epidemic dynamics in the absence of treatment beds. Gray line shows median number of cases generated from 1000 simulations of the fitted model, with 50% credible intervals given by dotted gray lines and 95% CI given by dashed lines. Blue line shows median community transmission rate, shaded area shows 95% credible interval (right hand axis). Black dots show weekly reported confirmed and probable cases in each district up to 2nd February 2015 (left hand axis).

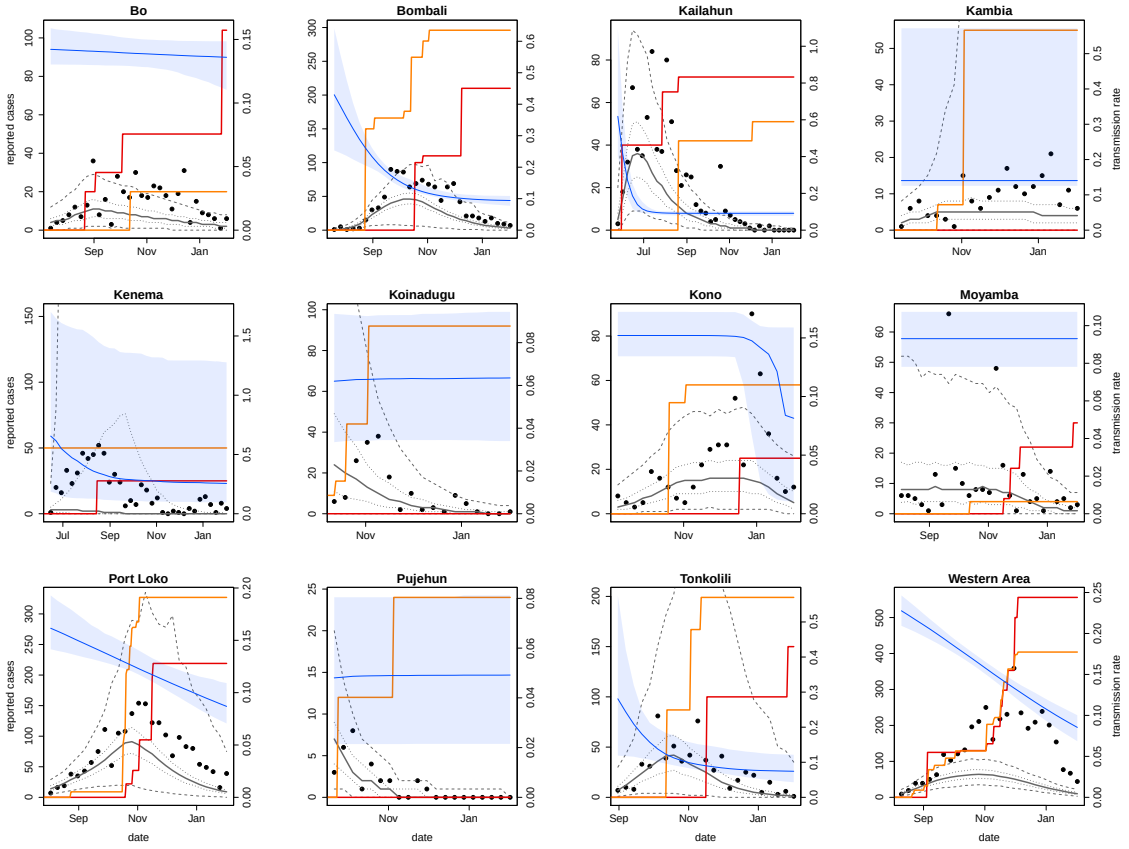

Figure S4: District-level epidemic dynamics when beds are introduced 4 weeks earlier. Gray line shows median number of cases generated from 1000 simulations of the fitted model, with 50% credible intervals given by dotted gray lines and 95% CI given by dashed lines. Blue line shows median community transmission rate, shaded area shows 95% credible interval (right hand axis). Black dots show weekly reported confirmed and probable cases in each district up to 2nd February 2015 (left hand axis). Solid red line, ETU bed capacity; orange line, EHC/CCC bed capacity.

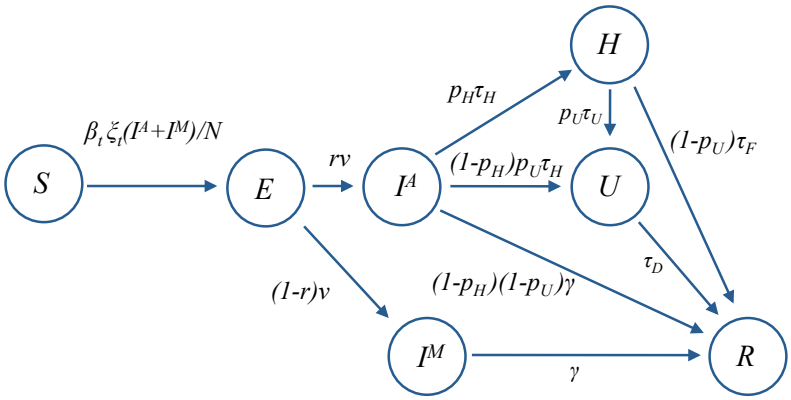

Figure S5: Model structure. Individuals start off susceptible to infection (S). Upon infection with Ebola they enter an incubation period (E), then at symptom onset they become infectious; these individuals either eventually become ascertained (I^A) or do not (I^M). Individuals who are ascertained initially seek health care in EHC/CCCs (or ETUs if these are full); if no beds are available, they remain infectious in the community until the infection is resolved (R) i.e. they have recovered, or are dead and buried. Patients in EHC/CCCs are transferred to ETUs once they have been tested for Ebola, which takes an average of 2 days. Patients remain in ETUs until the infection is resolved. We assume the latent period is 9.4 days, the average time from onset to EHC/CCC attendance is 4.6 days, and individuals who do not seek treatment are infectious for 11.3 days on average[1].

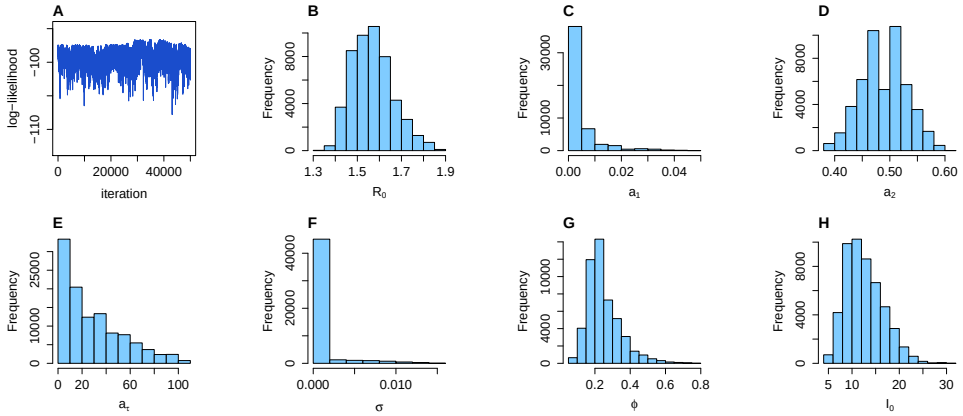

Figure S6: Estimated posterior parameter distributions for Bo. (A) MCMC trace plot of log-likelihood. (B) Basic reproduction number at the start of the outbreak in the district, $R_0 = \beta_0/\gamma$. (C) Slope of the time-varying transmission rate sigmoid, a_1. (D) Final value of sigmoid, a_2. (E) Midpoint of sigmoid, a_τ. (F) Volatility of transmission noise, σ. (G) Reporting error, ϕ. (H) Initial number of infectious individuals, I_0.

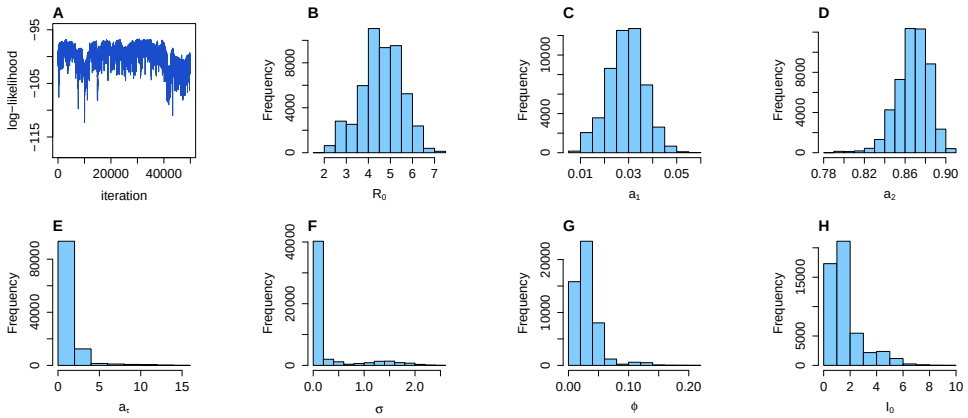

Figure S7: Estimated posterior parameter distributions for Bombali. (A) MCMC trace plot of log-likelihood. (B) Basic reproduction number at the start of the outbreak in the district, $R_0 = \beta_0/\gamma$. (C) Slope of the time-varying transmission rate sigmoid, a_1. (D) Final value of sigmoid, a_2. (E) Midpoint of sigmoid, a_τ. (F) Volatility of transmission noise, σ. (G) Reporting error, ϕ. (H) Initial number of infectious individuals, I_0.

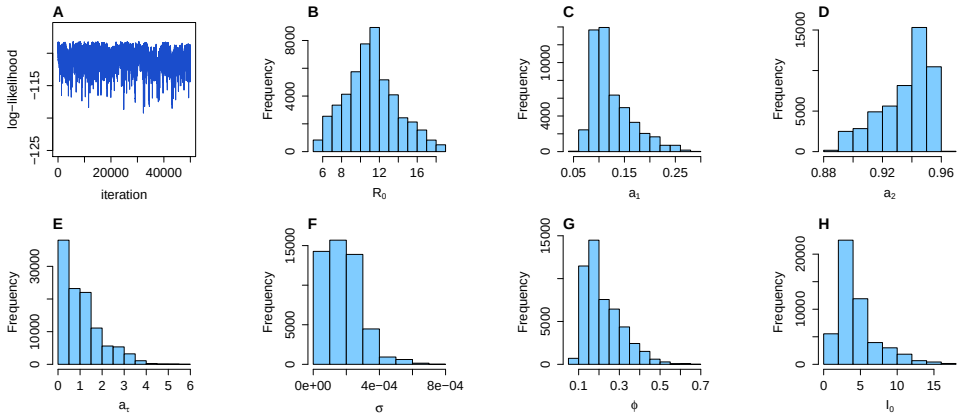

Figure S8: Estimated posterior parameter distributions for Kailahun. (A) MCMC trace plot of log-likelihood. (B) Basic reproduction number at the start of the outbreak in the district, $R_0 = \beta_0/\gamma$. (C) Slope of the time-varying transmission rate sigmoid, a_1. (D) Final value of sigmoid, a_2. (E) Midpoint of sigmoid, a_τ. (F) Volatility of transmission noise, σ. (G) Reporting error, ϕ. (H) Initial number of infectious individuals, I_0.

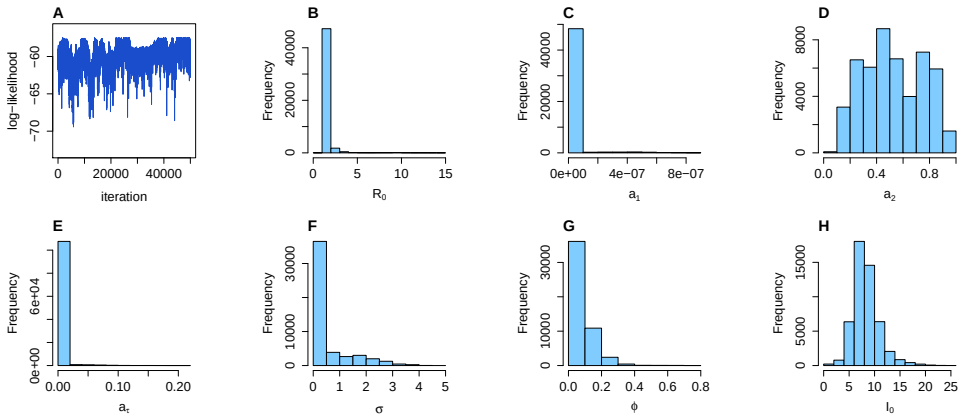

Figure S9: Estimated posterior parameter distributions for Kambia. (A) MCMC trace plot of log-likelihood. (B) Basic reproduction number at the start of the outbreak in the district, $R_0 = \beta_0/\gamma$. (C) Slope of the time-varying transmission rate sigmoid, a_1. (D) Final value of sigmoid, a_2. (E) Midpoint of sigmoid, a_τ. (F) Volatility of transmission noise, σ. (G) Reporting error, ϕ. (H) Initial number of infectious individuals, I_0.

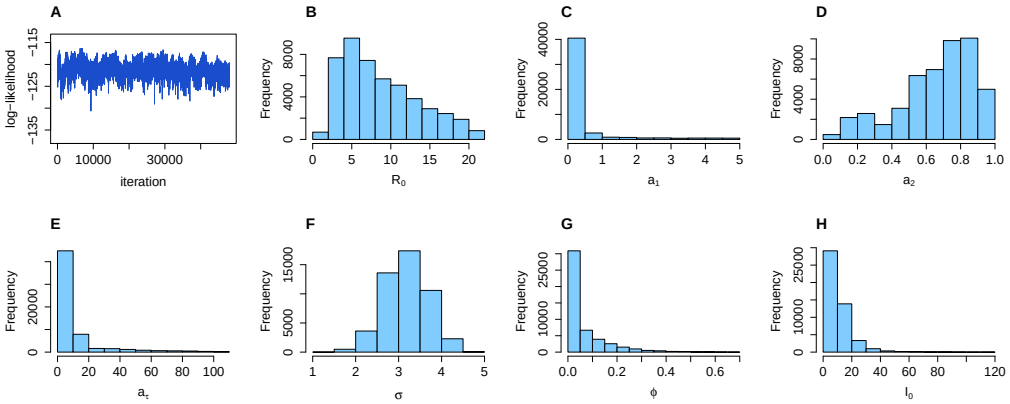

Figure S10: Estimated posterior parameter distributions for Kenema. (A) MCMC trace plot of log-likelihood. (B) Basic reproduction number at the start of the outbreak in the district, $R_0 = \beta_0/\gamma$. (C) Slope of the time-varying transmission rate sigmoid, a_1. (D) Final value of sigmoid, a_2. (E) Midpoint of sigmoid, a_τ. (F) Volatility of transmission noise, σ. (G) Reporting error, ϕ. (H) Initial number of infectious individuals, I_0.

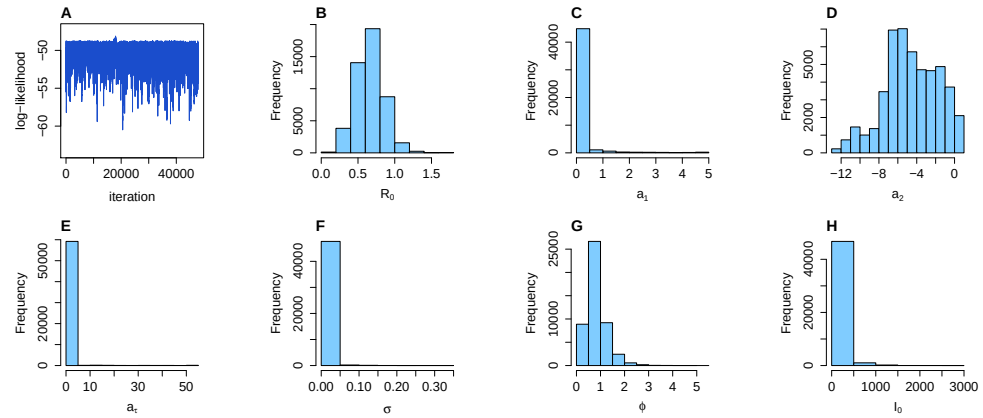

Figure S11: Estimated posterior parameter distributions for Koinadugu. (A) MCMC trace plot of log-likelihood. (B) Basic reproduction number at the start of the outbreak in the district, $R_0 = \beta_0/\gamma$. (C) Slope of the time-varying transmission rate sigmoid, a_1. (D) Final value of sigmoid, a_2. (E) Midpoint of sigmoid, a_τ. (F) Volatility of transmission noise, σ. (G) Reporting error, ϕ. (H) Initial number of infectious individuals, I_0.

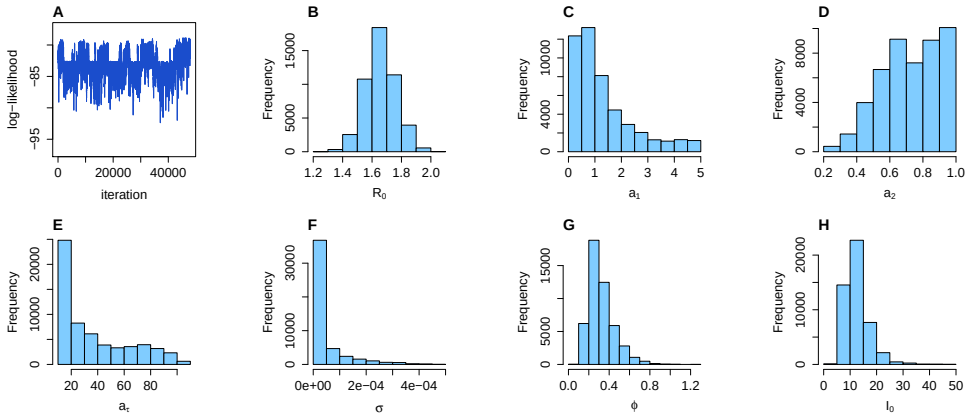

Figure S12: Estimated posterior parameter distributions for Kono. (A) MCMC trace plot of log-likelihood. (B) Basic reproduction number at the start of the outbreak in the district, $R_0 = \beta_0/\gamma$. (C) Slope of the time-varying transmission rate sigmoid, a_1. (D) Final value of sigmoid, a_2. (E) Midpoint of sigmoid, a_τ. (F) Volatility of transmission noise, σ. (G) Reporting error, ϕ. (H) Initial number of infectious individuals, I_0.The bimodal distribution of the log-likelihood is the result of the two peaks in epidemic time series; the model switches between these peaks when fitting the sigmoid, which leads to the broad posterior distribution for a_τ.

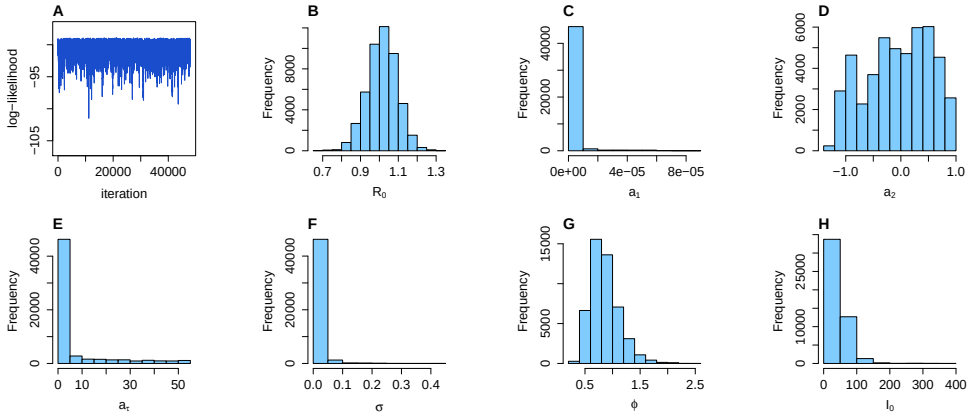

Figure S13: Estimated posterior parameter distributions for Moyamba. (A) MCMC trace plot of log-likelihood. (B) Basic reproduction number at the start of the outbreak in the district, $R_0 = \beta_0/\gamma$. (C) Slope of the time-varying transmission rate sigmoid, a_1. (D) Final value of sigmoid, a_2. (E) Midpoint of sigmoid, a_τ. (F) Volatility of transmission noise, σ. (G) Reporting error, ϕ. (H) Initial number of infectious individuals, I_0.

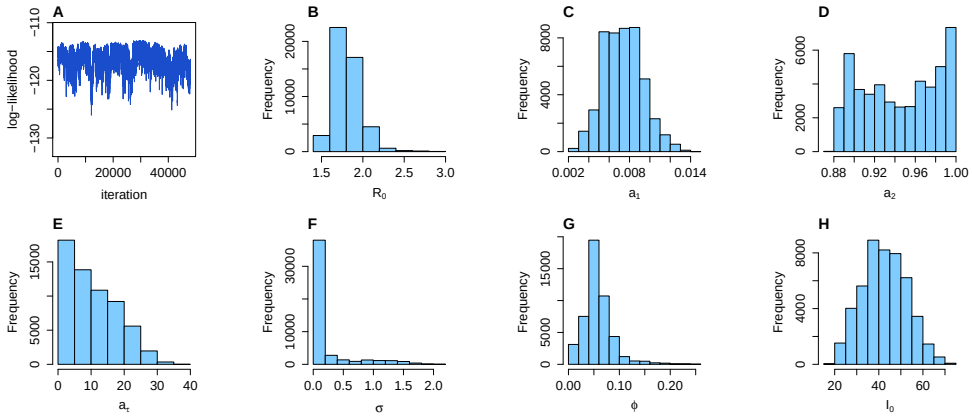

Figure S14: Estimated posterior parameter distributions for Port Loko. (A) MCMC trace plot of log-likelihood. (B) Basic reproduction number at the start of the outbreak in the district, $R_0 = \beta_0/\gamma$. (C) Slope of the time-varying transmission rate sigmoid, a_1. (D) Final value of sigmoid, a_2. (E) Midpoint of sigmoid, a_τ. (F) Volatility of transmission noise, σ. (G) Reporting error, ϕ. (H) Initial number of infectious individuals, I_0.

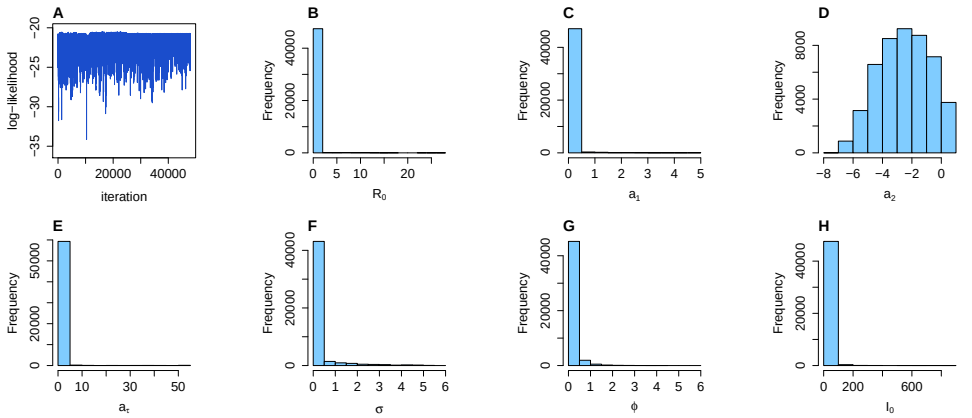

Figure S15: Estimated posterior parameter distributions for Pujehun. (A) MCMC trace plot of log-likelihood. (B) Basic reproduction number at the start of the outbreak in the district, $R_0 = \beta_0/\gamma$. (C) Slope of the time-varying transmission rate sigmoid, a_1. (D) Final value of sigmoid, a_2. (E) Midpoint of sigmoid, a_τ. (F) Volatility of transmission noise, σ. (G) Reporting error, ϕ. (H) Initial number of infectious individuals, I_0.

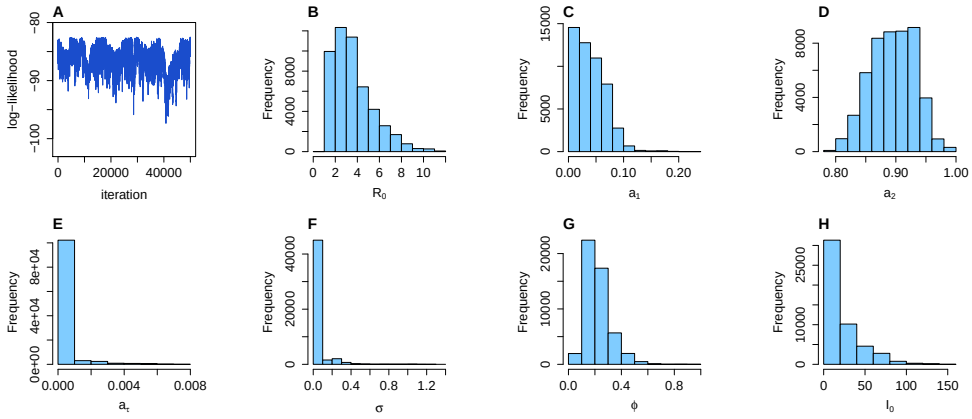

Figure S16: Estimated posterior parameter distributions for Tonkolili. (A) MCMC trace plot of log-likelihood. (B) Basic reproduction number at the start of the outbreak in the district, $R_0 = \beta_0/\gamma$. (C) Slope of the time-varying transmission rate sigmoid, a_1. (D) Final value of sigmoid, a_2. (E) Midpoint of sigmoid, a_τ. (F) Volatility of transmission noise, σ. (G) Reporting error, ϕ. (H) Initial number of infectious individuals, I_0.

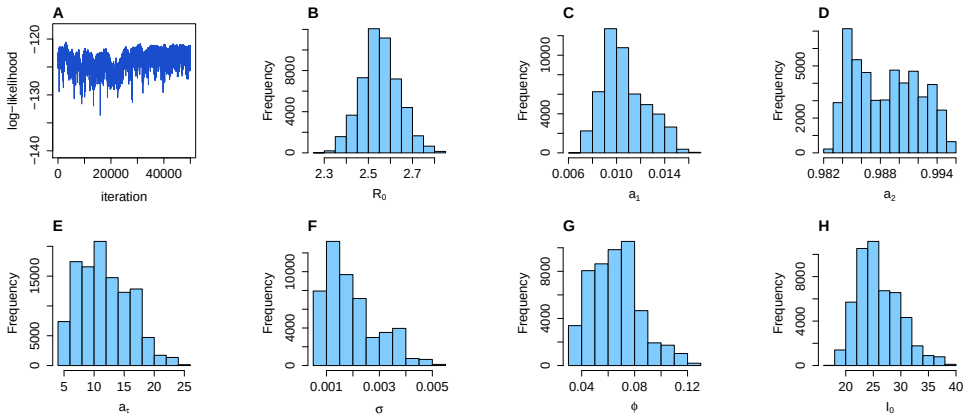

Figure S17: Estimated posterior parameter distributions for Western Area. (A) MCMC trace plot of log-likelihood. (B) Basic reproduction number at the start of the outbreak in the district, $R_0 = \beta_0/\gamma$. (C) Slope of the time-varying transmission rate sigmoid, a_1. (D) Final value of sigmoid, a_2. (E) Midpoint of sigmoid, a_τ. (F) Volatility of transmission noise, σ. (G) Reporting error, ϕ. (H) Initial number of infectious individuals, I_0.